

Effects of high energetic He^+ ion irradiation on the structure of polymeric hydrogenated amorphous carbon

Q. Zhang^{a,*}, S.F. Yoon^a, J. Ahn^a, Rusli^a, H. Yang^a, C. Yang^b, F. Watt^b, E.J. Teo^b,
T. Osipowice^b

^aMicroelectronics Centre, Nanyang Technological University, Singapore, Singapore

^bNuclear Microscopy Group, Department of Physics, National University of Singapore, Singapore, Singapore

Accepted 11 January 1999

Abstract

The effects of 2 MeV He^+ ion irradiation on the structure of polymeric hydrogenated amorphous carbon films were studied. It was found that after the irradiation up to a dose of $1.0 \times 10^{16} \text{ cm}^{-2}$, the carbon network transforms from a polymer-like to a diamond-like structure, as evidenced using Raman spectroscopy. Correspondingly, the optical band gap shrinks from 3.0 to 2.0 eV and the refractive index increases from 1.5 to 1.7. The processes of dehydrogenation and carbon rebonding into hydrogen-free $\text{C}(\text{sp}^3)$ and $\text{C}(\text{sp}^2)$ clusters under the impact of the incident ions are suggested to account for the carbon structural transformation. © 1999 Elsevier Science Ltd. All rights reserved.

Keywords: He^+ ion irradiation; Dehydrogenation; Carbon rebonding

1. Introduction

The modification of the properties of amorphous hydrogenated carbon (a-C:H) and diamond-like a-C:H films using high energetic ion implantation has been intensively investigated [1]. With the implantation of high energetic ions, such as H^+ , C^+ , N^+ , Ar^+ , Xe^+ , F^+ and Au^+ into a-C:H films beyond a critical dose of about 10^{14} – 10^{15} cm^{-2} , the conductivities of these irradiated films were found to increase dramatically [1–7]. Above the critical dose, most of the atoms in the irradiated area have on the average been dislodged once and hydrogen release from the films becomes significant. During this structural modification, a number of dangling bonds are produced through the breakage of C–C and C–H bonds [8] and the dangling bonds may provide a variable hopping tunnel for carriers, leading to a dramatic increase in the conductivity [1,2]. It has been reported that a significant improvement in the hardness of hydrogen-free a-C films was achieved using C^+ ion implantation [9–11]. The stress-driven forces and energy, as well as the momentum transferred to the carbon network by the C^+ ion implantation has been suggested to be the basis for densification associated with the disintegration of the sp^2 bonded carbon cluster and enhancement of the sp^3 -rich carbon structure [11]. Besides the earlier mentioned

structural variations, changes in the optical properties of the a-C:H films occur concurrently with high energetic ion implantation. The optical bandgap of a-C:H films was observed to reduce with increasing He^+ , C^+ , N^+ and F^+ ion dose [2,7,12,13]. This phenomenon was found to be related to the ion-implantation induced hydrogen removal which may directly cause a transformation from $\text{C}(\text{sp}^3)\text{-H}_n$ to $\text{C}(\text{sp}^2)$ clusters [1]. Other complementary findings, using IR absorption and Raman scattering, for the a-C:H films irradiated by high energetic H^+ , He^+ and N^+ ions do support the suggestion of the transformation from $\text{C}(\text{sp}^3)\text{-H}_n$ ($n = 1, 2$ and 3) to $\text{C}(\text{sp}^2)$ clusters [4,5,14].

In fact, the effects of high energetic ion implantation on the properties of a-C:H films depend strongly on the characteristic of the initial a-C:H films. Most of these intensive investigations mentioned earlier were actually performed on diamond-like carbon films which show a higher hardness, a smaller bandgap of about 1.5–1.7 eV and a higher ratio of $\text{C}(\text{sp}^3)$ to $\text{C}(\text{sp}^2)$. In this article, we present the results on 2 MeV He^+ ion irradiation induced change in the optical properties of soft, wide bandgap and more polymer-like carbon films.

2. Experimental conditions

The a-C:H film used in this study was prepared using the ECR–CVD technique. Upon introducing a mixture of

* Corresponding author.

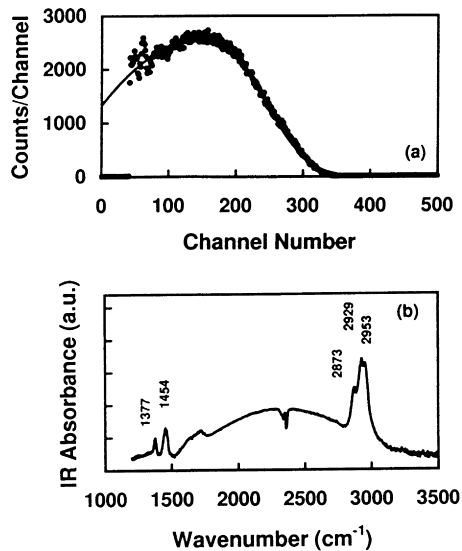


Fig. 1. ERDA spectrum (a), and FTIR spectrum (b) for the as-deposited a-C:H film.

10 sccm pure methane and 100 sccm hydrogen into the chamber, the plasma for the film deposition was excited in the ECR zone by feeding microwave at 2.45 GHz [15]. The substrate was only heated by the plasma during film growth and the substrate temperature was found not to exceed 60°C. No intended DC bias voltage was applied to the sample holder and the plasma induced DC bias voltage on the holder was about a few volts. Prior to deposition the chamber was pumped down below 5×10^{-6} Torr using a turbo molecular pump. The film was prepared under a constant microwave power of 600 W, pressure of 23 mTorr on $\langle 100 \rangle$ -oriented single crystal silicon.

The 2 MeV He^+ ion irradiation and elastic recoil detection analysis (ERDA) measurements were performed using a nuclear microscope which was based around a HVEC AN2500 single ended Van de Graaff accelerator [16]. The operating pressure was about 10^{-6} Torr. The irradiation was performed under two doses of 1.2×10^{15} and $1.0 \times 10^{16} \text{ cm}^{-2}$ at an incidence angle of 12° . To prevent excessive sample temperature rise during irradiation, the ion current intensity was controlled at 10^{-8} A/cm^2 . The temperature of the irradiated area was estimated to be below 200°C. For ERDA measurement, the incidence angle of the 2 MeV He^+ ion beam and the emission angle with respect to the sample surface were both 12° .

Raman scattering measurement, excited by an Ar^+ laser (514.5 nm), was carried out using the Ranishaw micro-Raman spectrometer. The ellipsometer (Uvisel) was employed to evaluate the optical properties of the films. The film thickness and its variation were measured using the Dektak surface profiler. It was found that the thickness measured using the profiler was consistent with that deduced using the ellipsometer. The thickness of the as-deposited film was about 1.3 μm .

3. Results and discussion

It is well known that many properties of a-C:H films are strongly influenced by their hydrogen content. The concentration of hydrogen in our as-deposited film was monitored using ERDA, as shown by the solid dots in Fig. 1(a). The ERDA data evaluation was carried out using SIMNRA code [17], as shown by the solid curve in Fig. 1(a), indicating that the atomic percentage of hydrogen was around 42 at.%. It has been proposed that at such a high hydrogen concentration, a-C:H films should be composed of sp^3 , sp^2 and sp^1 hybridized carbon atoms and most of the hydrogen atoms could bond to sp^3 hybridized carbon atoms or stay as hydrogen molecules in the voids in the film [18]. The appearance of the IR absorption bands at 1377, 1454, 2873, 2929 and 2953 cm^{-1} (see Fig. 1(b)) provide evidences for the existence of the hydrocarbon bonding configurations, because these bands are attributed to $\text{C}(\text{sp}^3)\text{-H}_3$ and $\text{C}(\text{sp}^3)\text{-H}_2$ vibration modes. In the high hydrogen content polymer-like carbon film, up to 80% of sp^3 bonded carbon atoms are expected to be hydrogenated and the number of $\text{C}(\text{sp}^3)\text{-H}$ could be factors of 1.6 and 5.7 larger than the numbers of $\text{C}(\text{sp}^3)\text{-H}_2$ and $\text{C}(\text{sp}^3)\text{-H}_3$, respectively [18].

The high energy of incident He^+ ions is transferred to the target carbon and hydrogen atoms through two dominant mechanisms. One is called electronic energy transfer (or electronic stopping) which happens when the incident He^+ ions interact with the electrons of the target carbon and hydrogen atoms. The other is nuclear energy transfer (or nuclear stopping) which is involved in the interaction between He^+ and the target atoms and becomes significant when the He^+ ions are slowed down at the end of the He^+ trajectories [1,19]. According to TRIM simulation, more than 90% of the ion energy from the MeV He^+ ions is transferred through electronic stopping, while nuclear stopping only takes strong effect at the end of the trajectories. Roughly assuming that the electronic energy transfer proceeds homogeneously over the projected mean range of about 7 μm in this type of an a-C:H film, we can estimate that the electronic energy loss (defined as the energy deposition per unit length along the ion track) was of the order of 30 $\text{eV}/\text{\AA}/\text{ion}$.

It has been suggested that under the impact of high energetic ions, if two C–H bonds are broken within a short characteristic distance from each other within a short time compared to the lifetime of free hydrogen atoms in the irradiated a-C:H films, the two hydrogen atoms may recombine to form hydrogen molecules and then diffuse out of the films [20]. It was reported that hydrogen loss is a universal process and MeV heavy ion (less than 0.25 MeV/amu) or sub-MeV light ion implantation shows a similar dependence for hydrogen concentration on implantation dosage [20]. If the effective hydrogen release cross section for the electronic energy loss of 30 $\text{eV}/\text{\AA}/\text{ion}$ and the saturated volume hydrogen concentration are taken as typical values of 0.4 \AA^2 and 5 at.%, respectively, then using the model

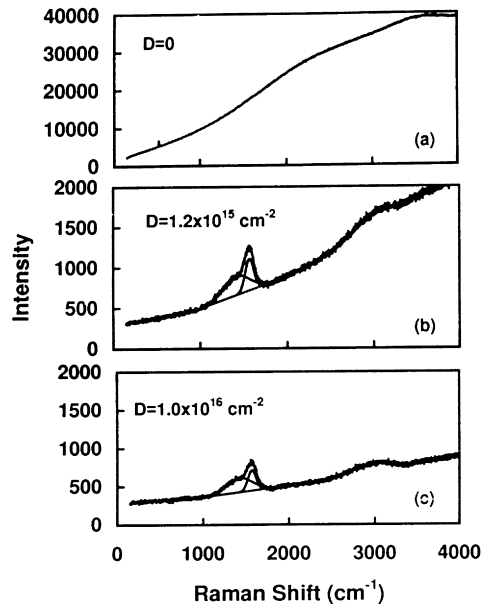


Fig. 2. Raman spectra of the a-C:H film before He^+ ion irradiation (a). The Raman scattering band at $1400\text{--}1600\text{ cm}^{-1}$ appears after the irradiation with doses of $1.2 \times 10^{15}\text{ cm}^{-2}$ (b) and $1.0 \times 10^{16}\text{ cm}^{-2}$ (c), respectively.

proposed by Adel et al. [20] one may estimate that the hydrogen content could be reduced to 30 at.% for a dose of $1.2 \times 10^{15}\text{ cm}^{-2}$ He^+ irradiation. However, up to a dose of $1.0 \times 10^{16}\text{ cm}^{-2}$ the hydrogen content is expected to be about 12 at.% or in other words more than two-third of the hydrogen atoms are likely to be released from the film. The hydrogen loss in a high energy condition ($\geq 0.5\text{ MeV/amu}$), under which the ERDA is performed, is still under investigation. The results will be published in a forthcoming article.

Hydrogen atoms bonded to the carbon network are

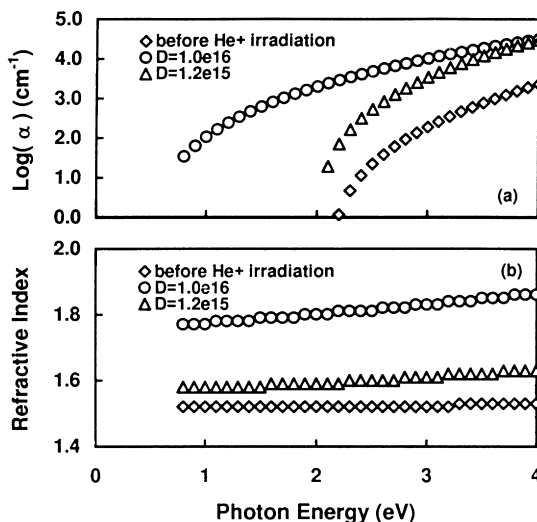


Fig. 3. The He^+ ion irradiation induced changes in optical coefficient (a), and refractive index (b) of the a-C:H film. The doses of the He^+ ion irradiation are indicated.

believed to play an important role in saturating the carbon dangling bonds and softening the carbon network. A significant loss of hydrogen creates a number of carbon dangling bonds which in turn could bond together under the impact of deposited extra energy, resulting in a structural change. The structural change due to the He^+ ion irradiation was monitored using Raman scattering, as shown in Fig. 2. Before the irradiation, except for a small silicon characteristic peak at 520 cm^{-1} , there is an absence of any carbon related Raman scattering band, see Fig. 2(a). A strong and smooth background increasing with wavenumber indicates that the photoluminescence signal excited by the Ar^+ laser (514 nm) dominates the measuring range. Taking the high hydrogen concentration and soft characteristics into account, we suggest that the a-C:H film possesses a polymer-like carbon structure [15]. However, after He^+ irradiation, the background is decreased dramatically and a Raman scattering band at $1400\text{--}1600\text{ cm}^{-1}$ and its second order scattering peak at around 3000 cm^{-1} are detected, see Fig. 2(b) and (c). This scattering band can be decomposed into two Gaussian peaks, i.e. ‘D’ peak at 1442 cm^{-1} and ‘G’ peak at 1572 cm^{-1} , as shown in solid curves in Fig. 2(b) and 2(c). The D and G peaks are assigned to the scattering of the disorder activated optical zone-edge phonons [21] and to the optical allowed E_{2g} zone center mode of crystalline graphite [22], respectively. With increasing irradiation dosage from 1.2×10^{15} to $1.0 \times 10^{16}\text{ cm}^{-2}$, the intensity ratio of the D peak to G peak I_D/I_G changed from 1.8 to 2.1. These values of I_D/I_G are comparable to those of typical hard DLC films. However, an increase in the I_D/I_G from 1.8 to 2.1 reflects that the ratio of sp^3 to sp^2 coordinated carbon decreases. It should be pointed out that in most cases an increase in the sp^3/sp^2 ratio corresponds to a decrease in the I_D/I_G ratio together with the downward shift of the D and G peak and an increase in the full-width at half maximum (FWHM) of the G peak [23,24]. However, in the present case the positions and widths of both the peaks do not show any detectable variations. For the G peak FWHM of about 113 cm^{-1} , we note that the FWHM is larger than those for normal hydrogenated DLC, but in the range of those for hard hydrogen-free DLC [24]. However, the effect of C–H bonds on the Raman spectra can be clearly identified in terms of an absence of the 600 cm^{-1} Raman peak, which, attributed to the Raman-inactive acoustic and out-of-plane optical vibrational modes of graphite [25,26], could appear in the Raman spectra for hydrogen-free DLC films [24].

The changes in the absorption coefficient and refractive index were monitored using an ellipsometer. It can be seen from Fig. 3(a) that the He^+ ion irradiation has dramatically enhanced the absorption coefficient α . It was increased by more than one order of magnitude at the photon energy of 4.0 eV after a dose of $1.0 \times 10^{16}\text{ cm}^{-2}$ He^+ ion irradiation. The optical bandgap deduced from the Tauc plot is found to reduce from 3.0 (as-deposited) to 2.5 eV for a dose of $1.2 \times 10^{15}\text{ cm}^{-2}$ and 2.0 eV for $1.0 \times 10^{16}\text{ cm}^{-2}$. These results are qualitatively consistent with other observations with hard

DLC films [2,7,12,13], as mentioned in Section 1. In addition, the refractive index was increased, as shown in Fig. 3(b), and the film thickness was correspondingly decreased by about 20–30%. The film shrinking characteristic is quite different from the report by Paterson et al. [14] where the He⁺ implanted DLC films was found to increase the film thickness. To our knowledge, the variation in refractive index has so far not been reported.

As mentioned before, the electronic stopping is a dominant process of energy deposition from the high energetic incident ions in the target a-C:H film. The interaction of the He⁺ ions and a-C:H film results in an ionization volume in which the target atoms are excited or ionized so as to break some of the C–H and C–C bonds. The released hydrogen atoms and some small hydrocarbon units could re-combine together to form hydrogen molecules or even methene molecules and diffuse out of the irradiated film. Therefore a number of carbon dangling bonds would be produced. This could account for the dramatic increase in the absorption coefficient. The carbon dangling bonds may rebond, under the influence of the extra deposited energy, to form a more stable carbon network. The structural change directly leads to the changes in the Raman spectra and optical bandgap. We propose that the micromechanisms for the bond transformation under the impact of high ion energy could be similar to those happening in thermal annealing [27]. These microprocesses could include, for example, a formation of C=C bonds from C–C bonds {Reaction (a): $6C(sp^3)-C(sp^3) \rightarrow C(sp^2) = C(sp^2) + 4C(sp^3)-(sp^2)$ } and a formation of H₂ from sp³-H_n {Reaction (b): $2C(sp^3)-H \rightarrow C(sp^3)-C(sp^3) + H_2$ }. Reactions (a) and (b) are endothermic with energies of about 0.11 and 0.49 eV, respectively. Hydrogen loss from the irradiated film may also realize through a formation of methane {Reaction (c): $4C(sp^3)-H + 6C(sp^3)-C(sp^3) \rightarrow CH_4 + C(sp^2) = C(sp^2) + 4C(sp^3)-C(sp^2)$ } with an endothermic energy of 0.14 eV which is actually smaller than that to form a hydrogen molecule. With hydrogen release and the creation of hydrogen-free C(sp³)-C(sp²) bonding clusters, the photoluminescence efficiency was reduced and the Raman scattering band at 1400–1600 cm⁻¹ was activated, as shown in Fig. 2(b). When the processes proceed, more and more C(sp²)=C(sp²) bonds are simultaneously produced so that they could rearrange into the bigger size of C(sp²) atom rings. This is believed to be the reason for the optical bandgap shrinking [28]. As the newly reformed carbon structure is denser than the initial polymer-like structure, the irradiated film has contracted, leading to an increase in the refractive index and a decrease in the film thickness. The film contraction is in some sense consistent with our thermal annealing results where the a-C:H film thickness was found to decrease with increasing annealing temperature and annealing time [29]. However, it is worth pointing out that the variations in the properties of a-C:H films induced by high energetic He⁺ ion irradiation at a small ion flux density should possess some different characteristics from those

induced by thermal annealing. Once the high energetic He⁺ ions penetrate into the film, a cascade of secondary collisions are excited in the vicinity of the primary collision event, causing energy deposition on the carbon network around the ion track in a short time of $\sim 10^{-13}$ s. Therefore, the bonding rearrangement could only occur very locally, and then quench in a very short time if the irradiated ion flux is so small that the interaction among the incident He⁺ ions can be neglected. In contrast, thermal annealing provides a uniform thermal energy distribution and carbon bonding rearrangement in the entire bulk of the films. In spite of these, thermal annealing is also a slow process in which bonding rearrangement proceeds in quasi-thermal equilibrium. As the He⁺ ion irradiation was performed at a temperature below 200°C and at a low pressure of 10⁻⁶ Torr, the structural modification which could be induced by thermal annealing during the irradiation can be neglected [29]. The different effects of He⁺ ion irradiation and thermal annealing on the carbon structure are now under investigation.

4. Conclusion

2 MeV He⁺ ion irradiation on a soft, polymer-like a-C:H films was investigated. Up to an irradiation dose of 1×10^{16} cm⁻², we found that the carbon network transforms from a polymer-like to a diamond-like structure; the optical band gap shrinks from 3.0 to 2.0 eV and the refractive index increases from 1.5 to 1.7. The creation of hydrogen-free C(sp³) and C(sp²) clusters due to dehydrogenation and carbon bond rearrangement under the impact of the deposited energy by the incident He⁺ ions are suggested to account for the transformation of the carbon network structure.

Acknowledgements

The authors would like to thank Mr. L.K. Cheah for the fitting of the ellipsometer spectra.

References

- [1] M.S. Dresselhaus, R. Kalish, *Ion Implantation in Diamond, Graphite and Related Materials*, Springer, Berlin Heidelberg, 1992.
- [2] S. Praver, R. Kalish, M.E. Adel, V. Richter, Effects of heavy ion irradiation on amorphous hydrogenated (diamond-like) carbon films, *J. Appl. Phys.* 61 (9) (1987) 4492–4500.
- [3] M. Rothschild, C. Arnone, D.J. Ehrlich, Excimer-laser etching of diamond and hard carbon films by direct writing and optical projection, *J. Vac. Sci. Technol.* B4 (1986) 310–314.
- [4] T. Wang, W. Wang, B. Chen, The irradiation effect of MeV protons on diamond-like carbon films, *Nucl. Instr. Meth. Phys. Res.* B71 (1992) 186–190.
- [5] W.J. Wang, T.M. Wang, C. Jing, Implantation effect of diamond-like carbon films by 110 keV nitrogen ions, *Thin Solid Films* 280 (1996) 90–94.
- [6] S. Sato, H. Watanabe, K. Takahashi, Y. Abe, M. Iwaki, *Electrical*

- conductivity and Raman spectra of C ion implanted diamond depending on the target temperature, *Nucl. Instr. Meth. Phys. Res. B* 59/60 (1991) 1391–1394.
- [7] S.P. Wong, S. Peng, N. Ke, P. Li, Effects of fluorine implantation into a-C:H thin films, *Diamond and Related Materials* 2 (1993) 580–583.
- [8] M.E. Adel, R. Kalish, S. Praver, *J. Appl. Phys.* 62 (1987) 4096.
- [9] A. Kolitsch, E. Richter, H. Drummer, U. Roland, J. Ullmann, The effects of a post-treatment of amorphous carbon films with high energy ion beams, *Nucl. Instr. Meth. Phys. Res. B* 106 (1995) 511–516.
- [10] N.J. Mikkelsen, S.S. Eskildsen, C.A. Straede, N.G. Chechenin, Formation of low friction and wear-resistant carbon coatings on tool steel by 75 keV, high-dose carbon ion implantation, *Surf. and Coat. Tech.* 65 (1994) 154–159.
- [11] A. Kolitsch, L. Sümmchen, J. Ullmann, U. Falke, P. Heger, Post-implantation of ions into amorphous carbon films, *Surface and Coatings Technology* 84 (1996) 495–499.
- [12] G.L. Doll, J.P. Heremans, T.A. Perry, J.V. Mantese, Optical and electronic properties of nitrogen-implanted diamond-like carbon films, *J. Mater. Res.* 9 (1) (1994) 85–90.
- [13] G. Compagnini, U. Zammit, K.N. Madhusoodanan, G. Foti, Disorder and absorption edges in ion-irradiated hydrogenated amorphous carbon films, *Phys. Rev. B* 51 (16) (1995) 11 168–11 171.
- [14] M.J. Paterson, K.G. Orrman-Rossiter, S. Bhargava, A. Hoffman, Physico-chemical changes in a-C:H by MeV He ion irradiation, *J. Appl. Phys.* 75 (2) (1994) 792–796.
- [15] S.F. Yoon, H. Yang, Rusli, J. Ahn, Q. Zhang, T.L. Poo, Influence of substrate temperature and microwave power on the properties of a-C:H films prepared using the ECR-CVD method, *Diamond Relat. Mater.* 6 (1997) 1683–1688.
- [16] F. Watt, I. Oelic, K.K. Loh, C.H. Sow, P. Thong, S.C. Liew, T. Osipowicz, T.F. Choo, S.M. Tang, The national university of Singapore nuclear microscope facility, *Nucl. Instr. Meth. Phys. Res. B* 85 (1994) 708–715.
- [17] M. Mager, SIMNRA User's Guide, Report IPP9/113, Max-Planck-Institut für Plasmaphysik, Garching, Germany, 1997.
- [18] H. Efsthiadis, Z.L. Akkerman, F.W. Smith, Atomic bonding in amorphous carbon alloys: a thermodynamic approach, *J. Appl. Phys.* 79 (6) (1996) 2954–2967.
- [19] W. Eckstein, Computer simulation of ion–solid interaction, Springer Ser. Mater. Sci., 10, Springer, Berlin Heidelberg, 1991.
- [20] M.E. Adel, O. Amir, R. Kalish, L.C. Feldman, Ion-beam-induced hydrogen release from a-C:H: a brk molecular recombination model, *J. Appl. Phys.* 66 (7) (1989) 3248–3251.
- [21] R.O. Dillon, J.A. Woollam, V. Katkanant, Use of Raman scattering to investigate diaorder and crystalline formation in as-deposited and annealed carbon films, *Phys. Rev. B* 29 (6) (1984) 3482–3489.
- [22] F. Tuinstra, J.L. Koenig, Raman spectrum of graphite, *J. Chem. Phys.* 53 (3) (1970) 1126–1130.
- [23] Rusli, S.F. Yoon, H. Yang, Q. Zhang, J. Ahn, Y.L. Fu, Effect of pressure on the deposition of a-C:H films using the ECR-CVD, *J. Vac. Sci. Technol. A* 16 (1998) 572.
- [24] M.A. Tamor, W.C. Vassell, Raman fingerprinting of amorphous carbon films, *J. Appl. Phys.* 76 (6) (1994) 3823–3830.
- [25] R. Al-Jishi, G. Dresselhaus, Lattice-dynamical model for graphite, *Phys. Rev. B* 26 (8) (1982) 4514–4522.
- [26] C. Oshima, T. Aizawa, R. Souda, Y. Ishizawa, Y. Sumiyoshi, Surface phonon dispersion curves of graphite (0001) over the entire energy region, *Solid State Commun.* 65 (1988) 1601.
- [27] Z.L. Akkerman, H. Efsthiadis, F.W. Smith, Thermal stability of diamond-like carbon films, *J. Appl. Phys.* 80 (5) (1996) 3068–3075.
- [28] J. Robertson, Structure and electronic properties of diamond-like carbon, in: R.E. Clausing, L.L. Horton, J.C. Angus, P. Koidl (Eds.), *Diamond and Diamond-like Films and Coatings*, Plenum Press, New York, 1990, pp. 331.
- [29] Q. Zhang, S.F. Yoon, Rusli, H. Yang, J. Ahn, Influence of oxygen on the thermal stability of a-C:H films, *J. Appl. Phys.* 83 (3) (1998) 1349–1353.